

Supporting Information

Advanced Janus Coatings for Thermal Management and Synergistic Flame Retardancy in Polyester Fabric

Liangyuan Qi ^{a,1}, Wei Cai ^{b,1}, Jiajun Li ^a, Tianyang Cui ^a, Liang Chen ^a, Jing Gao ^a, Bin Fei ^b, Yuan Hu ^a, Lei Song ^a, Zhou Gui ^{a*}, Weiyi Xing ^{a*}

^aState Key Laboratory of Fire Science, University of Science and Technology of China, Hefei, Anhui 230026, PR China

^bSchool of Fashion and Textiles, The Hong Kong Polytechnic University, Kowloon, Hong Kong SAR, 999077 China

*Corresponding authors

Tel/Fax:+86-0551-63600269;

E-mail addresses: zgui@ustc.edu.cn (Zhou Gui); xingwy@ustc.edu.cn (Weiyi Xing).

Characterization

Optical properties. The spectral reflectance $\rho(\lambda)$ and transmittance $\tau(\lambda)$ in the wavelength range of ultraviolet, visible light, and near-infrared (0.3~2.5 μm) were determined by polytetrafluoroethylene integrating sphere UV-Visible-near-infrared spectrophotometer (Hitachi U-4100, Japan). Infrared wavelengths in the range of rho (λ) integrating sphere with the gold of FTIR spectrometer (Nicolet6700 Thermo Fisher Scientific, USA) have been characterized. According to Kirchhoff's law, the spectral absorptivity ($\alpha(\lambda)$) and emissivity ($\varepsilon(\lambda)$) of any object in thermal equilibrium must be equal. Therefore, $\varepsilon(\lambda)=1-\rho(\lambda)-\tau(\lambda)$ ¹.

The average reflectance obtained by testing is required by further conversion. The conversion rules are as follows: STD-WS whiteboards with known absolute reflectance are regarded as standard whiteboards and are denoted as R0. The white board R1 is tested with its calibration, and the absolute reflectivity of the white board is R0*R1. Using the test board as the baseline, the reflectivity of the sample was measured as R2. Finally, the true reflectance of the sample is $R=R0*R1*R2$.

The average solar reflectivity (R_{Solar}) is defined as:

$$\bar{R}_{Solar} = \frac{\int_{0.3\mu m}^{2.5\mu m} I_{Solar}(\lambda) * R_{Solar}(\lambda, \theta) d\lambda}{\int_{0.3\mu m}^{2.5\mu m} I_{Solar}(\lambda) d\lambda}$$

Where λ is the wavelength of incident light in the range of 0.3-2.5 μm , I_{Solar} is the normalized ASTM G173 global solar intensity spectrum and R_{Solar} is the spectral reflectance of the coating surface.

The average emissivity ($\bar{\varepsilon}_{LWIR}$) in the long-wave infrared atmospheric transmittance window is defined as:

$$\bar{\varepsilon}_{LWIR} = \frac{\int_{8\mu m}^{13\mu m} I_{BB}(\lambda) * \varepsilon_{LWIR}(\lambda, \theta) d\lambda}{\int_{8\mu m}^{13\mu m} I_{BB}(\lambda) d\lambda}$$

Where, I_{BB} is the spectral intensity of blackbody emission, ε_{LWIR} is the angular spectral thermal emissivity of the coated textiles in the range of 8-13 μm .

Cooling characterization. The incubators consist of 33*33*35 cm³ insulated foam boxes covered with reflective foil. A transparent low-density polyethylene film is used to seal the incubator and act as a windscreen. In addition, some samples measuring 10*10*0.1 cm³ are placed in a groove at the top of the foam box, which is 1.3 m above the ground to avoid heat

conduction from the ground. The temperature detector is mounted directly on the back of the sample to detect the real-time temperature of the sample and is continuously recorded by a data recording thermometer with an uncertainty of ± 0.1 °C (I-7018, ICPDASCO., LTD., Taiwan, China). For comparison, a temperature detector was installed in the same location to detect the ambient temperature without the sample. Recording the solar radiometer (TES1333R, TES Electrical & Electronics, Taiwan, China) with an accuracy of $\pm 5\%$ while recording the solar radiation outside the box. On a clear day, the experiment was carried out on the flat roof of a five-story building at the University of Science and Technology of China in Hefei, China. September 9, 2023.

Heating characterization. The outdoor experiment was conducted in the same way as the cooling experiment. In addition, indoor simulated lighting experiments were also completed. Artificial light sources simulating 1000W/m² of sunlight were used to test the thermal management capabilities of the dual-mode textiles. Thermal infrared cameras were used to record the surface temperature of the textiles.

Characterization of the coating. ¹H NMR and ³¹P NMR were carried out at room temperature using CDCl₃ as a solvent on the AVANCE spectrometer (Bruker, Switzerland) at the frequency of 400 MHz. X-ray diffraction (XRD) is carried out at room temperature using an X-ray diffractometer equipped with a Cu-K α tube and a Ni filter. The morphology and structure of the samples were studied by scanning electron microscope (SEM) and an energy-dispersive X-ray analyzer (EDX). The surface of the samples was analyzed by JSM-6700F (JEOL). All samples are pretreated by spraying gold onto them to make the textiles' electrical conductivity. The XPS analysis was carried out on the PHI-TFAXPS spectrometer (Physical Electronics, Inc.).

Flame retardant characterization. The thermal stability of the treated cotton textiles was tested by a Q5000IR thermogravimetric analyzer (TA Instruments) at the heating rate of 20 °C/min in either an air or nitrogen atmosphere. Thermogravimetric analysis / infrared spectroscopy (TGA-FTIR) analysis of samples was carried out using a TGAQ5000IR thermogravimetric analyzer, which was interfaced with a Nicolet6700FT-IR spectrophotometer. The heating rate is set to 20 °C/min (in a nitrogen atmosphere, the flow rate is 55 mL/min). The Raman spectra of coke residues of samples with a wavenumber range of 800-2000 cm⁻¹ were obtained by SPEX-1403 laser Raman spectrometer (SPEX company, USA).

EnergyPlus simulation: The dual-mode RC/SH textiles cover onto the surface of the building model, excluding rooftop. The thickness of sample is 3.0 mm. The thermal conductivity, density, and specific heat capacity of sample are set as 0.05 W/mK, 0.0175 g/cm³, and 1.5

kJ/(kg*K) correspondingly. Haikou, Guangzhou, Shenzhen, Shanghai, Nanjing, Hefei, Chongqing, Beijing, Changchun, Lanzhou, Zhengzhou and Mohe were chosen as simulated cities.

Laundering durability test of coated samples was investigated via the AATCC test method 61(2A)-1996 in the presence of ECE non-phosphate standard detergent in ambient conditions at 38 ± 3 °C. Each cycle of the washing process is equivalent to home laundry five times. The durability of the coated fabric after 20 times washing was evaluated.

Coated textile moisture permeability performance concerning the standard GB/T12704.1-2009 "textile fabric moisture permeability test method" Part 1: moisture absorption method, choose condition A: temperature (38 ± 2) °C, relative humidity (90 ± 2) % for Coated textile moisture permeability test. Moisture permeability WVT ($\text{g}/(\text{m}^2 \cdot \text{h})$) is expressed as the average value of three specimens, and the result is retained with three effective digits according to GB/T12704.1-2009.

General purpose drawing machine (5565A Personal UK), used to test the tensile strength of Coated textiles. The tensile strength of textiles is tested according to the GB/T3923.1-2013 standard. The loading speed is 100 mm/min, and the textiles are cut into a size of 200*50 mm². The average of each sample is taken three times.

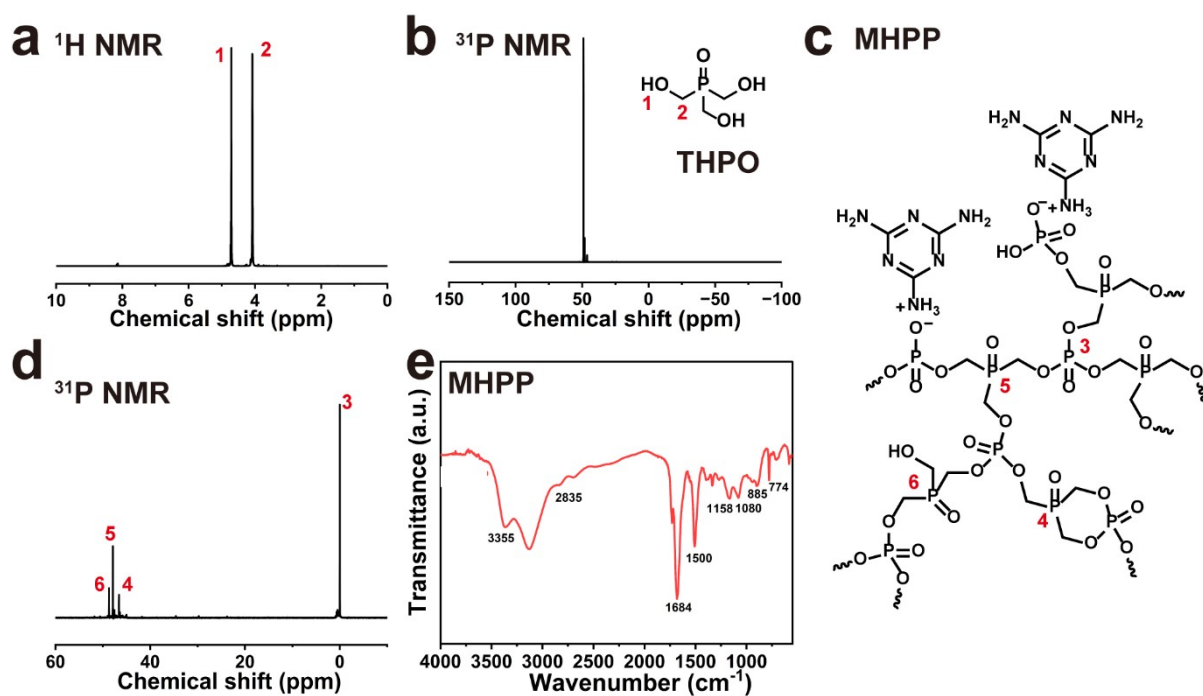


Figure S1. (a,b) The NMR spectra of THPO. (c) The chemical structure of MHPP. (d) The NMR spectra of MHPP. (e) The FTIR spectra of MHPP.

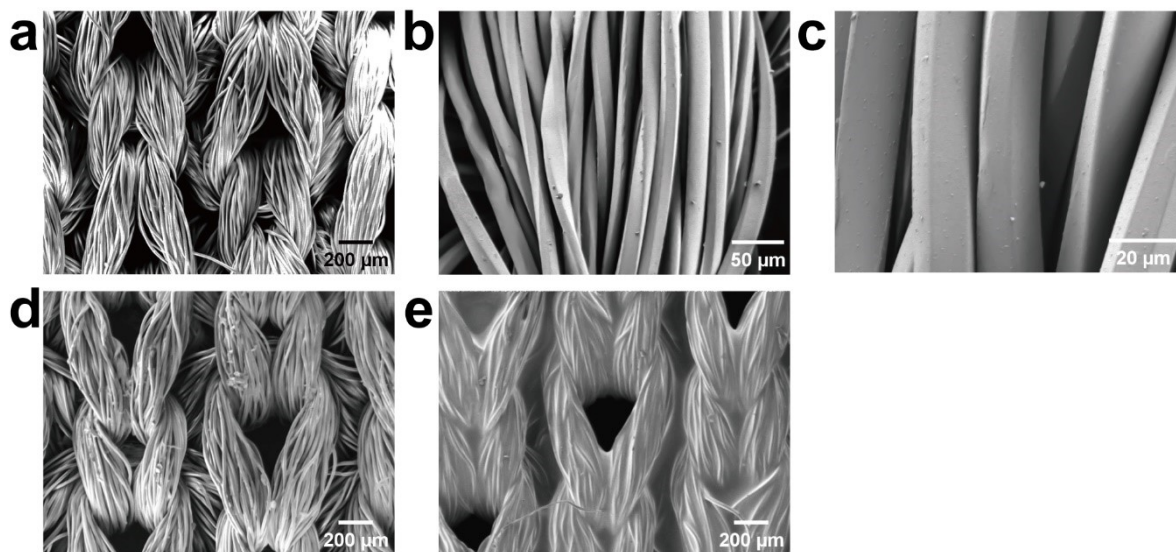


Figure S2. (a-c) The morphological pictures at different magnifications of pristine textiles. (d,e) The morphological pictures of PUC@MHPP and PUC@BP, respectively.

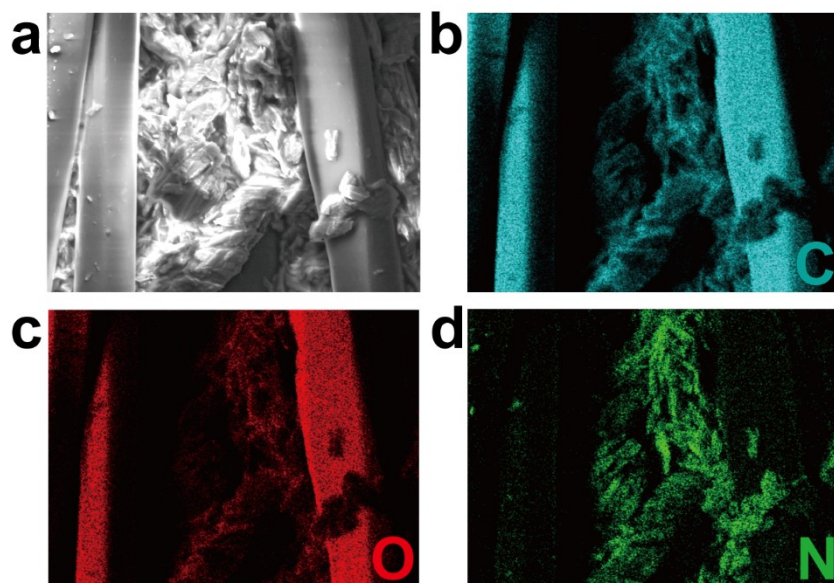


Figure S3. Distribution map of surface elements of PUC@MHPP.

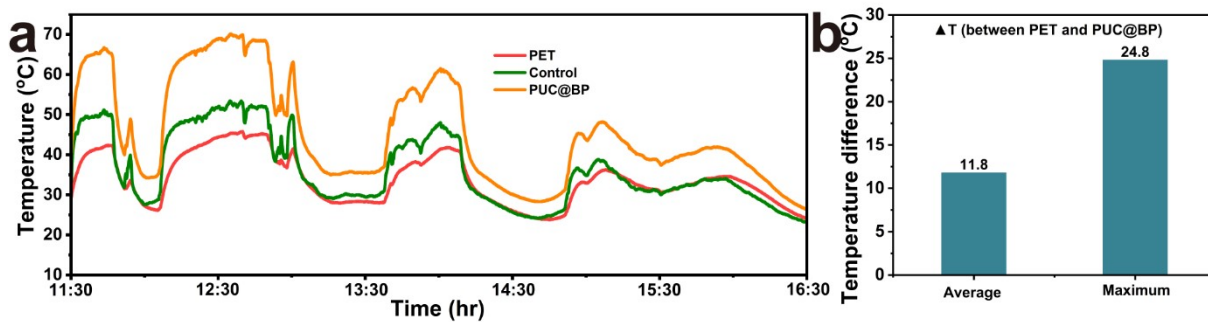


Figure S4. (a) the heating performance test curves of different textiles. (b) Average temperature difference and maximum temperature difference between cooling textiles and pure textiles.

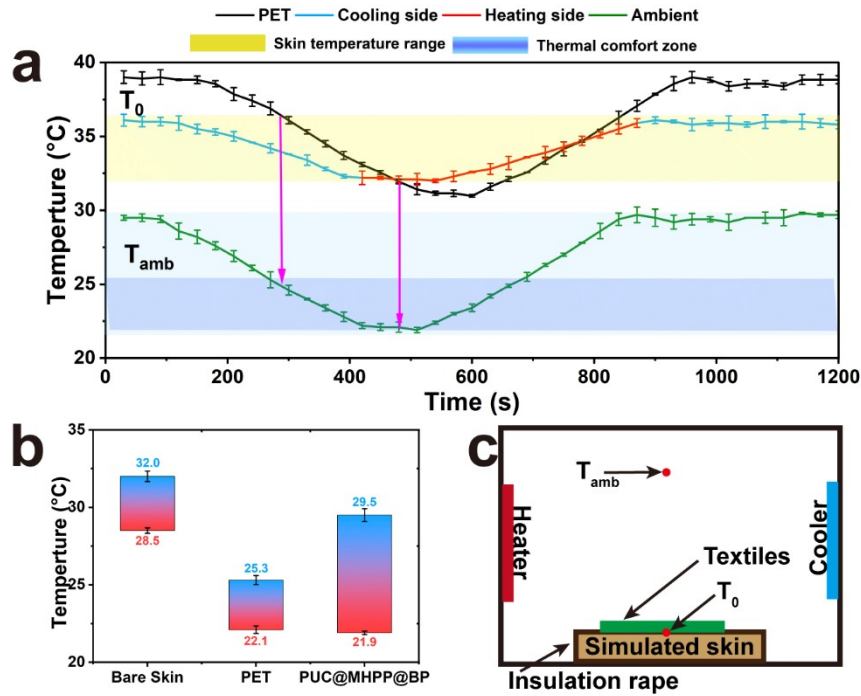


Figure S5. Measurement of thermal comfort zone. (a) Real-time thermal measurement of PUC@MHPP@BP and PET fabric under different ambient temperatures. (b) Thermal comfort zone of bare skin, PET textile, and dual-mode textile. (c) Side view of thermal measurement apparatus. By using cooling mode at high ambient temperature and heating mode at low temperature, the artificial skin temperature stays within 32 °C to 36 °C even if the ambient temperature changes between 21.9 °C and 29.8 °C. In contrast, the PET can only follow the trend of ambient temperature variation and result in thermal discomfort during the ambient temperature sweep. The error bars represent the SD of three measurements.

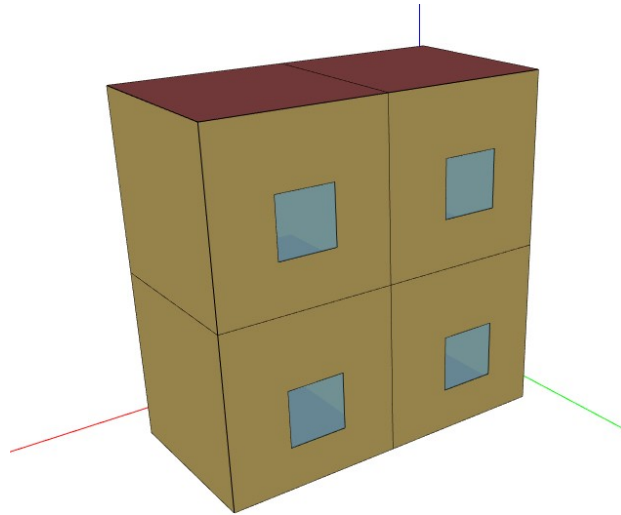


Figure S6. The office building model is used in the energy simulation.

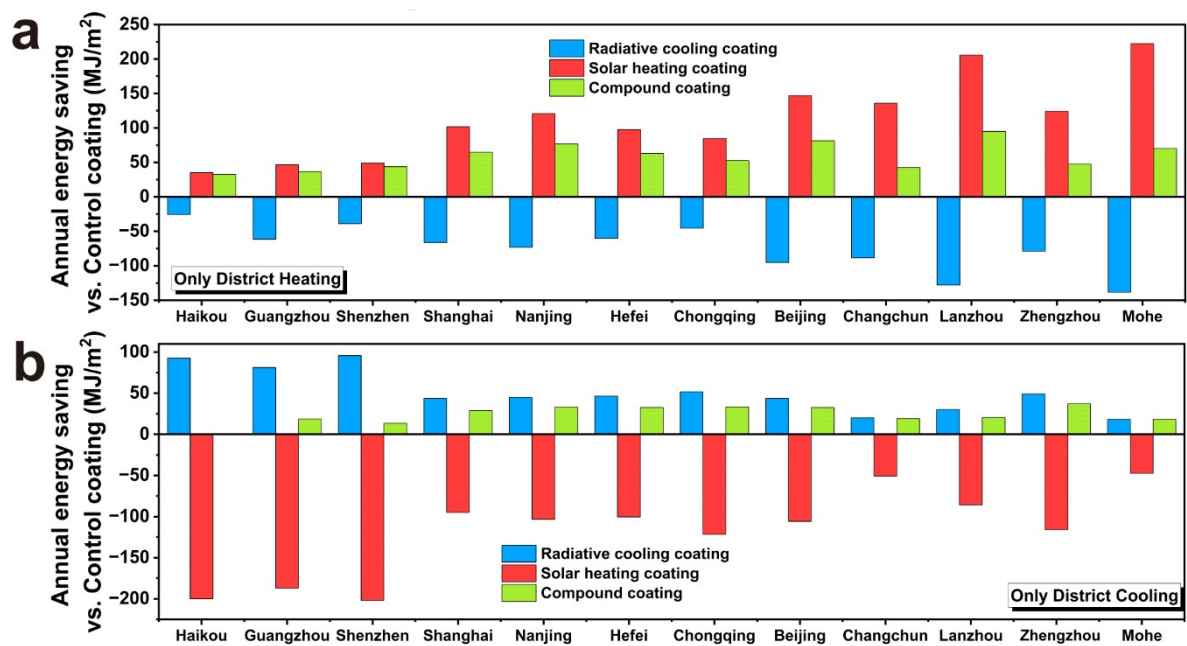


Figure S7. Energy consumption in different cities: only district heating (a), only district Cooling (b).

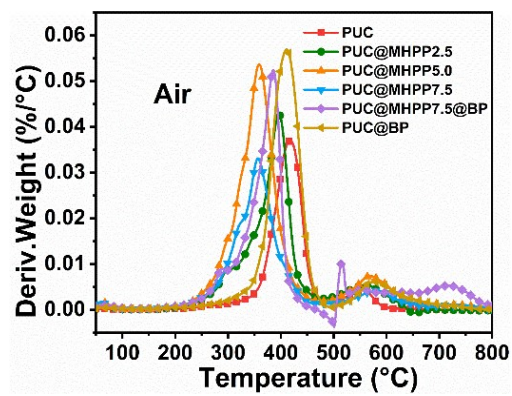


Figure S8. DTG curves of differently coated textiles

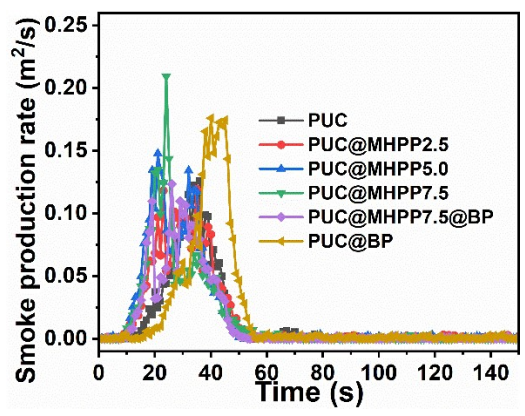


Figure S9. Smoke production rate versus time curves of coated textiles.

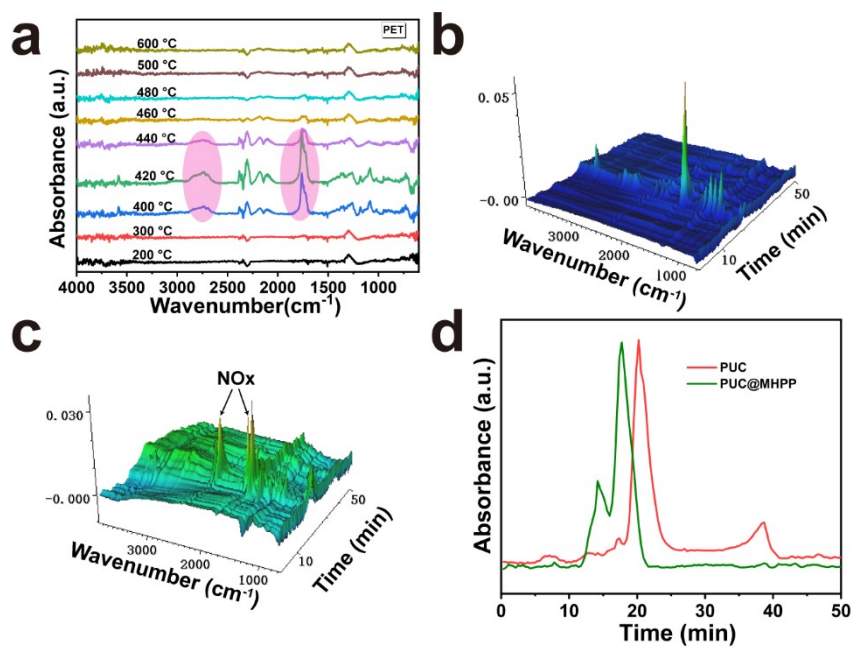


Figure S10. (a) Pyrolysis product curves of PET at different temperatures. (b, c) 3D images of pyrolysis products of PUC and PUC@MHPP. (d) Total pyrolysis product curve.

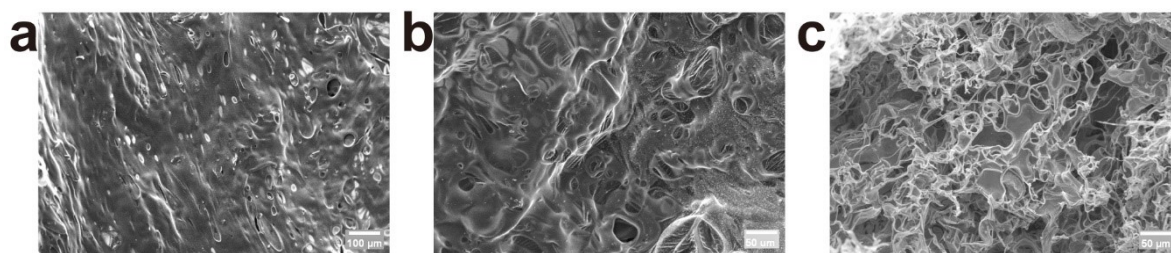


Figure S11. (a-c) Inner morphology images of carbon residues of PUC, PUC@MHPP, and PUC@MHPP@BP.

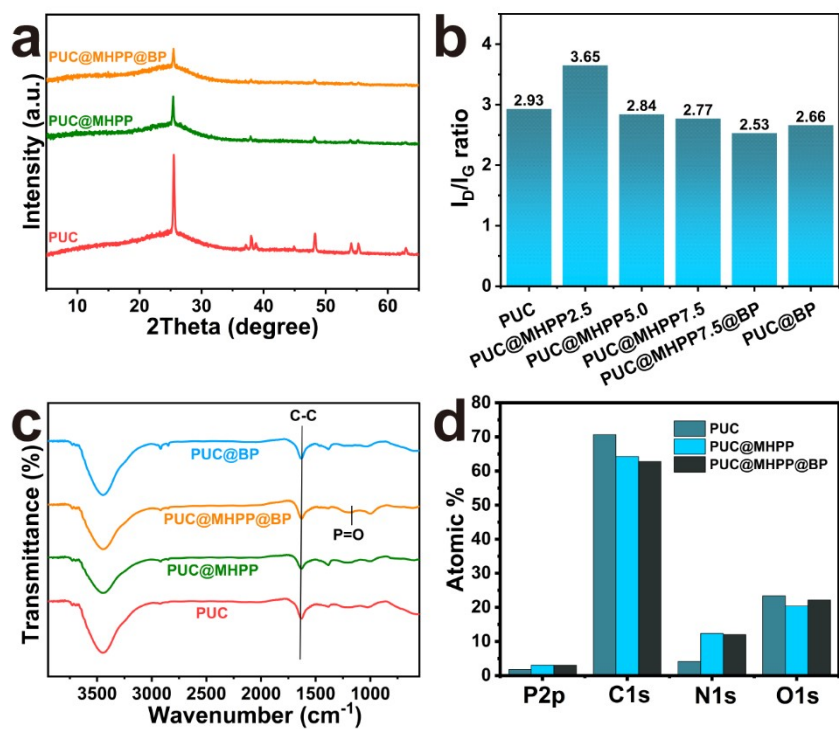


Figure S12. (a) XRD curve of char. (b) I_D/I_G of char. (c) FTIR curve of char. (d) XPS element proportion chart of char.

Table S1

Composition of different Coated textiles

Sample	PUC (wt%)	MHPP (wt%)	BP (wt%)	Thickness (mm)	Dual- mode or not	Thermal conductivity (W*m⁻¹*K⁻¹)
PET	/	/	/	0.600±0.0 05	No	0.092
PUC	100	/	/	0.206±0.0 10	No	/
PUC@MHPP2.5	97.5	2.5	/	0.749±0.0 31	No	/
PUC@MHPP5.0	95	5	/	0.741±0.0 45	No	/
PUC@MHPP7.5	92.5	7.5	/	0.758±0.0 13	No	/
PUC@MHPP7.5@BP	92.5/99.5	7.5	0.5	0.968±0.0 59	Yes	/
PUC@BP	99.5	/	0.5	0.832±0.0 36	No	/
PUC@MB-0.396	92.5/99.5	7.5	0.5	0.996±0.0 35	Yes	0.076
PUC@MB-0.561	92.5/99.5	7.5	0.5	1.161±0.0 65	Yes	0.068
PUC@MB-0.848	92.5/99.5	7.5	0.5	1.448±0.0 96	Yes	0.063

Table S2

Coated textile moisture permeability test data.

Sample	Method	Standard	g/m²•d
PET	Test method for water vapor permeability of textile fabrics Part 1: Moisture absorption method	GB/T 12704.1-2009 A	5856.3
			6159.8
			5769.5
			Average value
PUC@MB-0.396	Test method for water vapor permeability of textile fabrics Part 1: Moisture absorption method	GB/T 12704.1-2009 A	3956.8
			4356.9
			4259.8
			Average value
PUC@MB-0.561	Test method for water vapor permeability of textile fabrics Part 1: Moisture absorption method	GB/T 12704.1-2009 A	2359.6
			2054.3
			2200.8
			Average value
PUC@MB-0.848	Test method for water vapor permeability of textile fabrics Part 1: Moisture absorption method	GB/T 12704.1-2009 A	1953.8
			1638.5
			1768.3
			Average value

Table S3

Optical properties for samples used in energy simulation.

Optical properties	Control coating	Radiative cooling	Solar heating coating
Thermal absorptance	0.6	0.95	0.95
Solar absorptance	0.48	0.10	0.80
Visible absorptance	0.48	0.10	0.80

Table S4
Data related to energy-saving calculations.

City	Control coating		Radiative Cooling		Solar Heating		Cooling season (May.1-Oct.31)		Heating season (Nov.1-Apr.30)		Compound	
	District Cooling [GJ]	District Heating [GJ]	District Cooling [GJ]	District Heating [GJ]	District Cooling [GJ]	District Heating [GJ]	District Cooling [GJ]	District Heating [GJ]	District Cooling [GJ]	District Heating [GJ]	District Cooling [GJ]	District Heating [GJ]
Haikou	19.03	3.05	15.69	3.98	26.23	1.79	12.50	0.09	6.51	1.79	19.01	1.88
Guangzhou	15.16	5.29	12.24	7.50	21.89	3.62	10.71	0.38	3.78	3.59	14.49	3.97
Shenzhen	18.34	4.19	14.90	5.59	25.61	2.43	12.14	0.24	5.72	2.38	17.86	2.62
Shanghai	8.66	15.66	7.09	18.05	12.08	12.00	6.93	1.96	0.69	11.37	7.62	13.33
Nanjing	8.94	18.42	7.32	21.05	12.66	14.08	7.19	2.53	0.56	13.12	7.75	15.65
Hefei	9.29	17.94	7.62	20.12	12.91	14.43	7.36	2.00	0.76	13.67	8.12	15.67
Chongqing	9.44	13.72	7.58	15.36	13.82	10.67	7.22	1.92	1.02	9.91	8.24	11.83
Beijing	6.60	23.98	5.03	27.41	10.41	18.69	4.91	3.87	0.52	17.18	5.43	21.05
Changchun	3.08	41.50	2.36	44.69	4.91	36.61	2.35	7.62	0.04	32.32	2.39	39.96
Lanzhou	3.16	25.09	2.08	29.70	6.25	17.69	2.06	5.95	0.37	15.73	2.43	21.68
Zhengzhou	8.03	20.01	6.26	22.85	12.20	15.54	6.11	2.85	0.59	15.45	6.70	18.30
Mohale	1.94	61.59	1.29	66.57	3.65	53.59	1.29	14.09	0	44.98	1.29	59.07

Table S5

The TGA data of Coated textiles in air atmosphere

Sample	T_{-5%}(°C)	T_{-75 %}(°C)	T_{max1}(°C)	T_{max2}(°C)	Char (%)
PUC	334.2	434.9	417.6	554.2	1.75
PUC@MHPP2.5	278.1	411.5	395.6	554.6	0.51
PUC@MHPP5.0	272.3	394.5	358.9	568.5	1.36
PUC@MHPP7.5	257.8	397.0	356.8	582.1	2.12
PUC@MHPP7.5@BP	279.0	536.5	385.6	716.5	7.00
PUC@BP	330.6	434.5	411.0	574.4	1.44

Table S6
The LOI, vertical burning of Coated textiles.

	LOI (%)	LOI (%) after washing	Vertical burning test		
			After flame time (s)	Afterglow time (s)	Damaged length (mm)
PET	20.0±0.3	20.0±0.5	0	0	45
PUC	24.0±0.2	23.5±0.8	0	0	65
PUC@MHPP5.0	25.5±0.5	25.0±0.2	5	0	30
PUC@MHPP7.5	28.0±0.3	27.3±0.6	0	0	15

Table S7
Cone calorimetry data of Coated textiles.

Sample	TTI (s)	PHRR (kW/m²)	THR (MJ/m²)	Reduction in PHRR (%)	Char (%)
PUC	20±4	433±9	9.5±0.2	-	3.15
PUC@MHPP2.5	22±3	361±13	8.2±0.3	16.7	1.65
PUC@MHPP5.0	23±3	296±21	6.8±0.2	31.6	2.53
PUC@MHPP7.5	25±4	280±6	6.9±0.1	35.5	4.23
PUC@MHPP7.5@BP	18±1	259±7	7.5±0.1	40.1	7.65
PUC@BP	20±1	366±5	7.3±0.1	15.4	2.30

Table S8

Tensile properties of Coated textiles.

Samples	Tensile strength (MPa)	Elongation at break (%)
PET	16.8±0.68	72.6±5.6
PUC@MHPP2.5	23.8±0.25	110.8±3.1
PUC@MHPP5.0	23.1±1.81	102.0±5.1
PUC@MHPP7.5	22.1±1.60	105.1±5.8
PUC@MHPP7.5@BP	25.8±0.25	95.5±2.5

Table S9

The performance comparison of dual-mode textiles.

Samples	Material	Solar reflectivity (%)*	Emissivity (%)*	Stagnation temperature difference (°C)*	Self-extinguish	ref
HNF	PVB-PDMS/PAN-CNTs	92.2/19.9	90.4/69.9	7.2/12.2	/	2
Metafabric	PLA/Ag	87.6/-	94/41.3	6.5/3.5	/	3
PVDF-Al ₂ O ₃ /rGO-CB	PVDF-Al ₂ O ₃ /rGO-CB	92.2/5.6	96.9/8	5.3/17.8	/	4
LNT	PU-Al ₂ O ₃ -TF/PU-CB-FA	94.8/4.7	95/91.5	22/22.1	/	5
PUC@MHP P@BP	PUC-MHPP/PUC-BP	90/20	95.9/95	3.5/11.8	Yes	Present

*The cooling side/the heating side

References

1. A. Harrison, *Sol. Energy*, 1981, **26**, 243-247.
2. B. Gu, Q. Xu, H. Wang, H. Pan and D. Zhao, *ACS Nano*, 2023, **17**, 18308-18317.
3. X. Li, Y. Ji, Z. Fan, P. Du, B. Xu and Z. Cai, *Small*, 2023, **19**, 2300297.
4. X. Yang, Y. Yang, L. Chen, L. Zhu, W. Yu and Z. Zeng, *Chem. Eng. J.*, 2024, 152920.
5. N. Cheng, Z. Wang, Y. Lin, X. Li, Y. Zhang, C. Ding, C. Wang, J. Tan, F. Sun and X. Wang, *Adv. Mater.*, 2024, 2403223.